Exploring the applications of a pulsating jet hydrodynamic modulated voltammetric (HMV) system - electrochemistry of nanostructured Pt electrodes and trace analysis

Jekaterina Kuleshova[a], Peter R. Birkin[1a] and Joanne M. Elliott[b]

a School of Chemistry, University of Southampton, Southampton, SO17 1BJ United Kingdom

b Department of Chemistry, University of Reading, Reading, RG6 6AD, United Kingdom

Abstract

The electrochemistry of nanostructured electrodes is investigated using hydrodynamic modulated voltammetry (HMV). Here a liquid crystal templating process is used to produce a platinum modified electrode with a relatively high surface area (Roughness factor, Rf = 42.4). The electroreduction of molecular oxygen at a nanostructured platinum surface is used to demonstrate the ability of HMV to discriminate between faradaic and non-faradaic electrode reactions. The HMV approach shows that the reduction of molecular oxygen shows considerable hysteresis correlating with the formation and stripping of oxide species at the platinum surface. Without the HMV analysis it is difficult to discern the same detail under the conditions employed. In addition the detection limit of the apparatus is explored and shown, under ideal conditions, to be of the order of 45 nmol dm^{-3} employing $[Fe(CN)_6]^{4-}$ as a test species.

---

[1] Corresponding author, prb2@soton.ac.uk, tel: +44 2380 594172, fax: +44 2380 593781

Introduction

It is often the case, particularly for catalytic electrode reactions, that high surface area electrodes hold considerable benefit [1-5]. However, increasing the surface area of an electrode, while enhancing the catalytic reaction in question, will also increase background processes associated with the surface, double layer or oxide formation steps etc [6-8]. This imposes some limitations in the number of electrochemical techniques which are able to interrogate the reactions occurring. This is particularly true if dynamic experiments are advantageous (for example those where it is desirable to scan the potential of a high surface area electrode rapidly). Here we show how hydrodynamic modulated voltammetry [9, 10] (HMV) may be used to overcome some of these difficulties. This is a direct result of HMV offering the advantage of discrimination between solution phase Faradaic processes and non-Faradaic or surface bound Faradaic processes [11-14]. In particular we use HMV to investigate the important electrochemical reduction of molecular oxygen at a nanostructured [15] Pt electrode.

The fabrication and analytical applications of novel high surface area mesostructured microelectrodes produced by the 'true liquid crystal templating' technique have been widely reported, and these materials have been an area of interest for many authors [16-20]. Clearly the intrinsic high surface area of such electrodes can offer a significant advantage during the study of surface limited processes. However, the high surface areas can also be a disadvantage given the large currents associated with the electrochemical double layer, oxide and hydride processes. Consequently large background signals are associated with these electrodes. For example Birkin *et al.* showed that modified Pt microelectrodes, although catalytically

interesting for oxygen reduction, required relatively slow sweep rates (of the order of 2 mV s^{-1}) in order to observe the appropriate voltammetry in the absence of detrimental distortion [1].

The modulation of flow to investigate the HMV response of a system is not new. There are many examples of this technique within the literature. In brief they can be divided into two basic strategies. In the first, flow to the electrode can be modulated in a periodic manner. This may involve modulation of the rotation rate of a rotating disc electrode or alteration of the flow to an electrode by 'chopping' or oscillating the flow in a suitable manner [13, 14, 21, 22]. In the second, the modulation of the signal required is generated by the mechanical oscillation of an electrode [11, 12, 23]. Each of these systems has its advantages (for example the RDE system has known analytical solutions that may be applied to the system) and disadvantages (limited frequency regime and mechanical limitations) [11, 24-27]. Here we employ an oscillating jet as the method of hydrodynamic modulation. This system produces an HMV signal from a stationary jet/electrode arrangement. Here the system relies on positioning an electrode above a pulsating jet. In this case a small mechanical oscillation of a large membrane produced the desired periodic fluid motion. Amplification of this fluid motion was obtained using a conical section which enhances fluid flow at the jet orifice [28]. This system was shown to be reproducible and suitable for HMV studies. One major advantage of this system is that it is relatively simple and can be deployed for a large range of different electrode substrates. This communication shows how such an approach may be applied to a high

surface area electrode with significant catalytic interest and explores the detection limits achievable for a polished Pt interface.

Experimental

The general experimental arrangement used in this work has been reported previously [28]. Briefly this consisted of a ~3.5 cm radius membrane attached to the base of an inverted funnel. The funnel neck is then pulled into a 2 mm diameter jet orifice. In order to improve upon the previous performance of the system, the membrane was attached to a piston or disk like structure. This was designed to ensure complete motion of the membrane. A mechanical shaker (a Model V4, Signal Force, Data Physics Ltd) was attached to the centre of the piston which was glued to a viton (500 μm thickness, Altec Products Ltd) sheet which replaced the acetate membrane described in an earlier communication. This sheet was attached to both the base plate and the inverted funnel to act as a flexible seal. A mechanical coupling incorporating a single axis accelerometer (Model 3100B, Dytran Instruments, Inc., sensitivity 99.3 mV g^{-1}) was included in order to access the magnitude of motion of the piston. The accelerometer signal was conditioned with an amplifier (Model 4105C, Dytran Instruments, Inc.) and recorded on an oscilloscope (Techtronixs, TDS 2014, 1GS/s, 100 MHz). The shaker was driven by an amplifier (Signal Force 30W Power amplifier, Model PA 30E, Data Physics Ltd) which is in turn supplied by a function generator (TGA12101 100 MHz Arbitrary Waveform generator, TTi Ltd). In all cases the frequency of oscillation of the membrane, and hence jet, was 16 Hz. The electrodes employed (Pt, 0.5 mm) were fabricated in-house and were sealed in glass (diameter 5.0 mm). Positioning of the electrode with respect to the jet orifice was controlled using an XYZ stage (Zaber, 60 mm travel, resolution 0.1 μm, TLA 60A actuators connected to TSB 60-M stages). Data analysis (lock-

in experiments) and positioning was attained through in-house written software (VB6) [29].

For flow visualisation, a 50 µm diameter Pt wire (Advent RM) was stretched across the neck of the flow apparatus. Here an inverted funnel with the same jet dimensions was employed. However, the tip of the jet was cut off, the Pt wire stretched across followed by reattachment of the tip of the jet. Electrochemical hydrogen bubble generation was driven by a DC power supply and imaged using a Photron APX RS high-speed camera.

The electrodes were hand polished to a mirror like finish, in a conventional manner, using alumina powder slurries (Struers, alumina 0.3 µm diameter) on microcloth (Buehler) polishing pads. A three electrode system (using a mercury/mercurous sulphate, MMS, or Ag reference and Pt counter electrodes) was employed in the experiments. Electrochemical data was acquired on an in-house constructed potentiostat interfaced to a PC through an ADC card (Computer boards type PCI-DAS1602/16). Software, to determine either conventional cyclic voltammetry or the HMV signal, was developed in-house. A pump (TCS, micropump, Model M100-S) was also included in the experimental arrangement (note that this was only used for the titration experiments). The pump employed in the titration experiments was used to mix the dead volume of the lower conical section of the cell with the upper compartment and hence ensure an even concentration of the titrant throughout the cell after each appropriate addition into the upper chamber.

A schematic of the improved flow apparatus including the position of the pump and the microwire (used for high-speed tracking experiments) is shown in figure 1.

Solutions were prepared using a Purite Select Fusion 160 (Ondeo) water purification system (resistivity typically >15 MΩ cm and a TOC < 10 ppb). H$_2$SO$_4$ (98%, Fisher-Scientific), Sr(NO$_3$)$_2$ (99+%, Sigma-Aldrich) and K$_4$[Fe(CN)$_6$] (LRG, Fisher-Scientific) were used as received.

The Pt nanostructured electrode was deposited on a 0.5 mm diameter Pt disk electrode which had been previously electrochemically cleaned by cycling between +0.7 and -0.65 V *vs.* MMS at 200 mV s^{-1} in a 1 mol dm^{-3} sulfuric acid solution. The preparation of the mesoporous electrodes followed the procedure previously described [15]. Electrodeposition of the platinum films was achieved under potentiostatic and thermostatic control, the potential was stepped from +0.2 to -0.5V *vs.* MMS. After deposition (9.12 mC), the electrode was removed from the cell and allowed to soak in deionised water, which was regularly replaced in order to remove the surfactant. Voltammetry of the electrode in sulfuric acid was used to determine the roughness factor (187 immediately after preparation) of the electrode as described previously [30].

Results and discussion

Figure 2 shows two images gathered from high-speed camera investigations of the new 'piston cell. Here a 50 µm diameter Pt wire is suspended across the neck section ~1 cm below the 2 mm diameter jet. Hydrogen bubbles were electrochemically generated and can be seen scattering light.   In this experiment the oscillation of the fluid within the neck region of the flow apparatus can clearly be seen associated with bubble motion within the flow system.   The two frames shown are 31 ms apart corresponding to half the period of fluid oscillation employed in the HMV experiments described here and elsewhere.   The dotted horizontal lines indicate the displacement of the fluid noted from the bubble motion within the apparatus.   Under these conditions this corresponds to a zero-to-peak amplitude (labelled 'd' on figure 2) of 1.73 mm (determined using tracking analysis software).   This can be compared to the motion of the piston determined by an accelerometer placed within the mechanical coupling. The peak to peak displacement of the piston was under these conditions 0.0155 mm. This displacement can be compared to the fluid motion at the neck section of the flow apparatus by equating the volumes (taking into account the geometries involved).   The piston motion predicts a zero-to-peak amplitude of 1.76 mm at the neck section of the apparatus. This is in good agreement with the measured value determined from the high-speed camera data (see figure 2). This demonstrates that the refinement in the cell design (in particular the removal of the unsupported membrane) greatly improves the performance of the system (see reference [28]). In turn it is now possible to calculate the maximum velocity at the jet exit directly from the accelerometer data.   Under these conditions a jet

amplitude of 0.87 m s^{-1} is to be expected.   This HMV system was applied to two specific applications.   In the first we investigated nanostructured electrodes while in the second we explored trace analysis determination within this experimental setup.

Consider the application of an HMV system to the investigation of the catalytic activity of high surface area electrodes. Figure 3 (a) shows classic cyclic voltammetry of a nanostructured platinum electrode (0.5 mm diameter) recorded in the presence (J) and absence (NJ) of jet action. Figure 3 (a) is obtained by considering the time averaged current which in this case is plotted as a function of the electrode potential. Consider the case in the absence of the jet action (NJ).   Figure 3 (a) clearly shows that the voltammetry of polycrystalline Pt is observed [31]. Here hydrogen UPD peaks are apparent at potentials less than -0.4 V *vs.* MMS. It is clear that two peaks normally referred to as corresponding to 'strong' and 'weakly' bound H$_{UPD}$ can be seen [32, 33]. At more positive potentials (E > + 0.1 V *vs.* MMS) the formation of platinum oxide can be observed [31, 34-36].   Stripping of this oxide on the reverse scan can be seen at ~0 V *vs.* MMS under these conditions. Note that this voltammetry is performed in the presence of molecular oxygen and as such one would expect a corresponding cathodic current to be recorded as soon as the potential of the electrode becomes sufficient to avoid oxide formation. However, little or no evidence for this process can be observed in the stagnant solution. This emphasises the characteristics of this electrode in conjunction with the experimental conditions employed in the voltammetry. The electrode has been modified with a nanostructured Pt surface [30] and a roughness factor (determined by standard electrochemical methods) of 42.4 is

present.   Hence the real surface area is 0.083 cm^2 and the Faradaic electrochemical signal for the reduction of molecular oxygen is considerably smaller than the electrochemical signal from the hydride, double layer and oxide processes described previously [1].   This is a consequence of the high surface area, the mass transfer characteristics present (here planar diffusion to a macroelectrode) and the voltammetric rate employed.   Note that previous voltammetry of Pt modified microelectrodes has shown the voltammetry of molecular oxygen on the electrode [1].   However, in this case the mass transfer characteristics where enhanced through the radial component present for the microelectrode and the voltammetry was performed at 2 mV s^{-1} where the current associated with surface processes are reduced by a factor of 10. However, the presence of the voltammetric signal for molecular oxygen reduction can be observed by perturbation of the mass transfer characteristics of the system.   Consider the case in the presence of jet action (see figure 3(a) (J)).   Under these conditions the time averaged signal recorded for the same electrode in the presence of the forced mass transfer resulting from the action of the oscillating jet is shown.   In this case the surface processes remain unchanged and are still clearly evident.   However, a clear cathodic signal due to the reduction of molecular oxygen at potentials less than ~ +0.1 V *vs.* MMS can be seen.   Unfortunately the voltammetry of molecular oxygen is still partially obscured by the surface electrochemistry of this modified electrode. This is unfortunate as important questions relating to the catalytic activity of the modified surface are difficult to answer under these circumstances.   For example it would be desirable to explore the exact potential at which the reduction of molecular oxygen 'turned on and off'.   It is not possible to clearly

discern this information from the data presented in figure 3 (a). However, as we will now show, it is possible to find this information from HMV analysis of the same system.

Consider the results presented in figure 3 (b). Here the locked in HMV data is shown in the absence (NJ) and presence (J) of the oscillating jet. This data was obtained using the experimental procedure described in detail previously [28]. Note that figure 3 (b) (NJ) is essentially zero over the complete voltammetric sweep. This indicates, as expected, that in the absence of pulsed flow induced by the action of the apparatus employed, no signal from the reduction of molecular oxygen, the H_{UPD}, double layer and platinum oxide contribute to the locked in signal. However, in the presence of the jet oscillation (see figure 3 (b) (J)) a clear cathodic wave is observed. This corresponds to the reduction of molecular oxygen at the platinum surface. Note that the oxide, double layer and H_{UPD} signals (all surface processes) are not observed. This is a key observation and a fundamental characteristic of the HMV technique. HMV relies on modulation of the liquid hence only electroactive material in solution (such as molecular oxygen) is affected by the pulsed action of the jet and the associated mass transfer perturbations. In turn these contribute to a pulsed electrochemical signal which, through the appropriate data analysis, is extracted as a clear voltammetric signal for reduction of molecular oxygen. Figure 3 (b) (J) clearly shows the potentials at which reduction of molecular oxygen is initiated on the Pt surface. Here this occurs at + 0.128 V *vs.* MMS with a corresponding half wave potential ($E_{1/2}$) of +0.034 V *vs.* MMS. A clear mass transfer limited potential region is observed below -0.2 V *vs.* MMS for this mesoporous electrode which is assumed to

correspond to the 4 electron reduction of molecular oxygen. The magnitude of this signal is ~ -2.57 µA and corresponds to the zero-to-peak amplitude of the current transients induced by the pulsating forced convection of material to the electrode surface. Turning to the reverse trace (when the potential is swept from -0.65 V *vs.* MMS to +0.7 V *vs.* MMS), the HMV data clearly shows a marked hysteresis between the forward and reverse scan. The 'turn off' potential for oxygen reduction is +0.258 V *vs.* MMS with a corresponding $E_{1/2}$ of +0.121 V *vs.* MMS. Hence there is a separation of ~90 mV in the forward and reverse half wave potentials. Presumably this corresponds to the hysteresis in the oxide formation and stripping observed for the platinum surface. Nevertheless without the ability of the HMV system to extract the relevant data from the experimental information, this observation is difficult to make from the conventional cyclic voltammetry because of the size of the current resulting from the surface processes under these conditions. This shows the ability of HMV to be used with this system and demonstrates that this approach will be useful in analysing other catalytic reactions at high surface area electrodes. In the absence of modulation, the HMV signal is essentially zero over the entire voltammetric range (see 'NJ' on figure 3 (b)) as expected. Lastly, in this section, if the oxygen concentration was increased or decreased the signal from the HMV analysis responded in the appropriate manner as expected.

The data gathered from the nanostructured electrode can be compared to the response recorded at a polished Pt electrode under similar conditions. Figure 4 shows the time averaged (a) and HMV data (b) gathered under these conditions. There are a number of differences between the responses of the

polished electrode compared to the response of the nanostructured electrode. First, the half wave potential for the polished electrode is significantly more negative when compared to the nanostructured electrode. For example the data shown in figure 4 (b) shows a half wave potential for molecular oxygen reduction of -0.167 V *vs.* MMS on the cathodic sweep of the voltammogram. This compares to +0.034 V *vs.* MMS for the corresponding trace on the nanostructured electrode (see figure 3 (b)). Second, the hysteresis between the reverse and forward scan is less dramatic compared to the nanostructured case. Third, the mass transfer limiting region is far less well defined for the polished electrode, of a smaller magnitude (note ~-1.4 µA compared to -2.57 µA for the nanostructured system) and shows greater hysteresis within the hydride region when compared to the same characteristics recorded for the nanostructured electrode. These observations are all indicative of the electrochemical behaviour associated with the reduction of molecular oxygen at a polished Pt surface. In the experimental setup deployed here, a forced convection regime is utilised. This, in association with the relatively low roughness factor of the polished Pt surface, results in a reduced apparent number of electrons for the reduction of molecular oxygen [37, 38], far greater potential dependence and a significant negative shift in the reduction potential. Finally it should be noted that the polished electrode response was particularly sensitive to surface preparation (as expected) while the nanostructured electrode (which was electrochemically cleaned by cycling in acid) exhibited far greater reproducibility from day-to-day experiments. Nevertheless these experiments have shown the advantages of the HMV system developed in this work particularly when investigating the response of

high surface area electrodes of the type and roughness factor reported here. Clearly, further work investigating the effects of changing the roughness factor surface roughness is of interest but these are beyond the scope of this paper and will be reported elsewhere. It should be emphasised that the system is relatively simple to construct and a variety of different conventional electrodes can be simply positioned above the jet.

While in the previous section the ability of the HMV system to investigate catalytically important modified electrodes has been highlighted, one of the well documented characteristics of HMV, namely its use as an electroanalytical tool for trace analysis investigation, remains to be reported. In this section we present some preliminary data that suggests that this particular experimental apparatus has promise for this application.

In order to perform trace analysis experiments, the apparatus had to be modified with the addition of a small pump. This is required as the apparatus has a considerable 'dead' volume which corresponds to the large conical section of the flow apparatus (see figure 1). This has a volume of ~ 70 cm^3. In order to perform sensible titration experiments, where the solution is well mixed throughout the entire cell, material was added to the top reservoir and then the entire cell solution pumped around for a predefined time while the jet was operational (in this case ~40 - 50 s, note the volumetric flow rate produced by the micropump deployed is quoted to be up to 350 cm^3 min^{-1}, hence this represents thorough mixing of the cell contents [39]). This ensures that the entire volume of the apparatus is well mixed. Trace analysis experiments were performed in an aerobic medium. These experimental conditions were chosen as they allow for the lock-in setup (see previous

report [28]) to be attained for the reduction of molecular oxygen at the Pt electrode employed. Hence an appropriate phase angle could be acquired for the chosen electrode position. This phase angle was then employed for further trace analysis experiments at an appropriate electrode potential to detect the particular species in question. In the results presented here, a test system consisting of the titration of $[Fe(CN)_6]^{4-}$ into the cell was selected. This system was chosen for a number of reasons. First, the electrochemistry of this particular species is known to be well behaved in the electrolyte solution employed [40]. Second, the electrochemical potential is well away from the electrochemical reduction of molecular oxygen at the Pt surface in this environment (note the mass transfer reduction of molecular oxygen at the Pt surface was found to occur at potentials < -0.6 V vs. Ag, while the electrochemical oxidation of the $[Fe(CN)_6]^{4-}$ species was undertaken at + 0.5 V *vs.* Ag). In addition to these advantages, in an effort to reduce background contributions to the system (note the titrations will be on the nmol dm^{-3} scale where trace electrolyte impurities will be of significance on a catalytically active material like Pt), the electrode potential of the Pt was chosen to minimise the HMV signal in the absence of the addition of the target species (specifically $[Fe(CN)_6]^{4-}$). However, the potential chosen (+ 0.5 V vs. Ag) corresponds to the mass transfer limited potential region for the $[Fe(CN)_6]^{4-}$ species. This is ideal as it allows for the additions of the $[Fe(CN)_6]^{4-}$ to be mass transfer limited and hence have their highest effect. Figure 5 shows a collection of results attained from the titration of two additions of $[Fe(CN)_6]^{4-}$ to produce concentration steps of 30 nmol dm^{-3} $[Fe(CN)_6]^{4-}$ in the cell. Figure 5 (a) shows the HMV signal plotted as a function of time. Panel 'A' corresponds

to the situation where the jet is running, the pump is off but no $[Fe(CN)_6]^{4-}$ has been added to the cell. Under these conditions a stable background current of ~ 32 pA (note scale) was recorded. T1 represents the first addition of $[Fe(CN)_6]^{4-}$ to the cell. This is followed by a pumping period (see figure 5 grey regions) required to mix the entire cell. Interestingly the disruption of the flow in the cell induced by the pump action causes the HMV signal to fall to essentially zero (indeed this is the case for all additions). When the pumping period was terminated the HMV current returns immediately to a stable but new level ~ 42 pA (see panel 'B'). This process is repeated at T2 for a further injection of material and mixing period. After each injection and mixing period the HMV signal recovers to a stable but progressively more positive value (for example ~52 pA after two additions). The concentration steps employed here were 30 nmol dm^{-3} hence we recorded ~ 0.33 pA $nmol^{-1}$ dm^3 changes in the signal. In order to calculate the limit of detection from this experiment we consider three times the standard deviation of the background signal and compare this to the current steps induced by the concentration additions [41]. This results in a detection limit for this system of the order of 45 nmol dm^{-3}. This is in the range expected for an HMV system [10]. However, further points can be made which highlight the advantages of this system over conventional electrochemical chronoamperometric analysis. For example figure 5 (b) shows the time averaged signal (I_{av}) acquired simultaneously with the HMV signal presented in figure 5 (a). Note that the signal for the time averaged current (I_{AV}) is much higher (as all components including background signals etc. will be recorded) as expected. However, the time average signal varies considerably over the time course of the experiment and

although the current can be seen to increase as expected on addition of the $[Fe(CN)_6]^{4-}$ to the cell, analysing this change is extremely difficult and unreliable as it requires a sampling time to be chosen. This is not the case with the HMV signal shown in figure 5 (a). Here the signal can be seen to stabilise immediately that the pump is terminated and remain constant for extended periods at a constant concentration of $[Fe(CN)_6]^{4-}$. This shows a significant advantage of the HMV system over conventional chronoamperometric detection. The low detection limit and hence sensitivity of the HMV system is not only impressive, but in addition it does not suffer from drifting background signals associated with the electrode measurement (particularly if, as stated here, the conditions are chosen to reduce background interference) under normal chronoamperometric conditions.

Conclusions

The modified HMV oscillating jet design has been demonstrated to be successful and in line with the expected fluid motion from the associated piston displacement.

The applications of this pulsating jet as a HMV system have been investigated in relation to the study of catalytic reactions at a nanostructured electrode and trace analysis at a polished electrode surface. First, it has been clearly shown that, under the conditions reported here, a clear voltammetric curve for the electroreduction of molecular oxygen at a nanostructured Pt electrode surface has been obtained. Second, this signal is obtained for a relatively large electrode (e.g. not a microelectrode) at a reasonably fast sweep rate (here 20 mV s^{-1}). Third, significant hysteresis between the forward and reverse scans, attributed to the differing potentials for oxide stripping and formation processes, have been observed. Fourth, the response of the nanostructured electrode is significantly different when compared to a polished surface.

Turning to the investigation of the detection limit attained from this apparatus, it has been shown that this is of the order of 45 nmol dm^{-3} for the $[Fe(CN)_6]^{4-}$ system employed. In addition, the signal was also shown to be stable and free from background drift observed for normal chronoamperometry. Hence this technique holds considerable promise for analytical investigations of both trace systems and catalytic reactions.

Acknowledgements

Figure Legends

Figure 1. Schematic representation of the HMV flow cell employed in this work adapted for titration experiments. Here a metal piston replaces the membrane arrangement reported previously. An accelerometer (A) was included between the minishaker (MS) and the piston. The position of the electrode with respect to the orifice of the jet was controlled by an XYZ stage. Note the position of the microwire for the flow visualisation experiments is included in the figure.

Figure 2. Two images showing the liquid displacement inside the neck of the flow apparatus as a result of modulation of the piston. This was recorded using a high-speed camera. The timescale between the images is 31 ms corresponding to the period of the piston modulation (16 Hz). The flow within the funnel was visualized using hydrogen bubbles generated electrochemically (current of 0.01 A) at a 50 μm diameter Pt wire stretched across the neck of the funnel (highlighted by ———). The extremes of fluid flow are also highlighted (— — —). The scale bar indicates 1 mm. Note '*d*' represents the measured displacement zero to peak amplitude. The flow system contained 0.1 mol dm^{-3} Sr(NO$_3$)$_2$.

Figure 3. Plot showing the time average current signal (I$_{av}$) and HMV signal (I$_{HMV}$) as a function of electrode potential recorded at 0.5 mm diameter nanostructured Pt electrode (RF = 42.4) in aerobic 1 mol dm^{-3} sulfuric acid solution. Note the experimental data was gathered with the jet on (J) or off (NJ). The sweep rate was 20 mV s^{-1}. The oscillating jet was modulated at a

frequency of 16 Hz and with a piston displacement amplitude (zero to peak) of 0.021 ± 0.001 mm. The temperature of the solution was 18-22°C.

Figure 4. Plot showing the HMV signal (I_{HMV}) and average current signal (I_{av}) as a function of electrode potential recorded at a 0.5 mm diameter polished Pt electrode (RF = 1.6) in aerobic 1 mol dm^{-3} sulfuric acid solution. Note the experimental data was gathered with the jet on (J) or off (NJ). The sweep rate was 50 mV s^{-1}. The oscillating jet was modulated at a frequency of 16 Hz and with piston displacement amplitude (zero to peak) of 0.028 ± 0.001 mm. The temperature of the solution was 18-22°C.

Figure 5. Plots showing the results of the titration experiments. T1, T2, T3 correspond to the titration points. The grey shaded areas correspond to the time periods when the micropump was operational. I_{HMV} and I_{av} are HMV and time averaged current respectively recorded as a functions of time. The working electrode employed was a polished 0.5 mm diameter Pt positioned at the edge of the jet with a vertical displacement of 1 mm. The electrode was held at a potential of +0.5 V *vs.* Ag. The concentration of $Fe(CN)_6^{4-}$ was changed from 0.0 in section 'A', to 30 nmol dm^{-3} in section 'B' and to 60 nmol dm^{-3} in section 'C'. The electrolyte solution used was aerobic 0.1 mol dm^{-3} $Sr(NO_3)_2$. At each titration (T1, T2, T3) 13 μmol dm^{-3} of 0.4 mmol dm^{-3} $Fe(CN)_6^{4-}$ was added to the electrolyte solution. The experiments were performed at room temperature 18-22 °C.
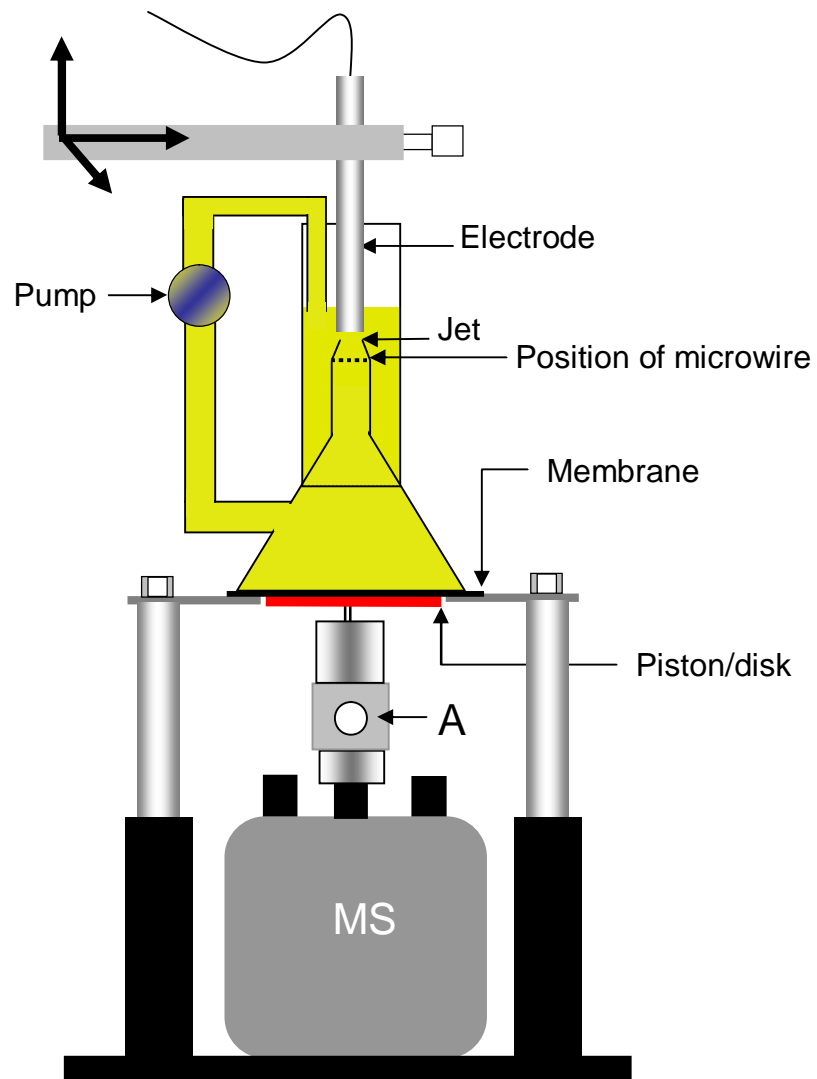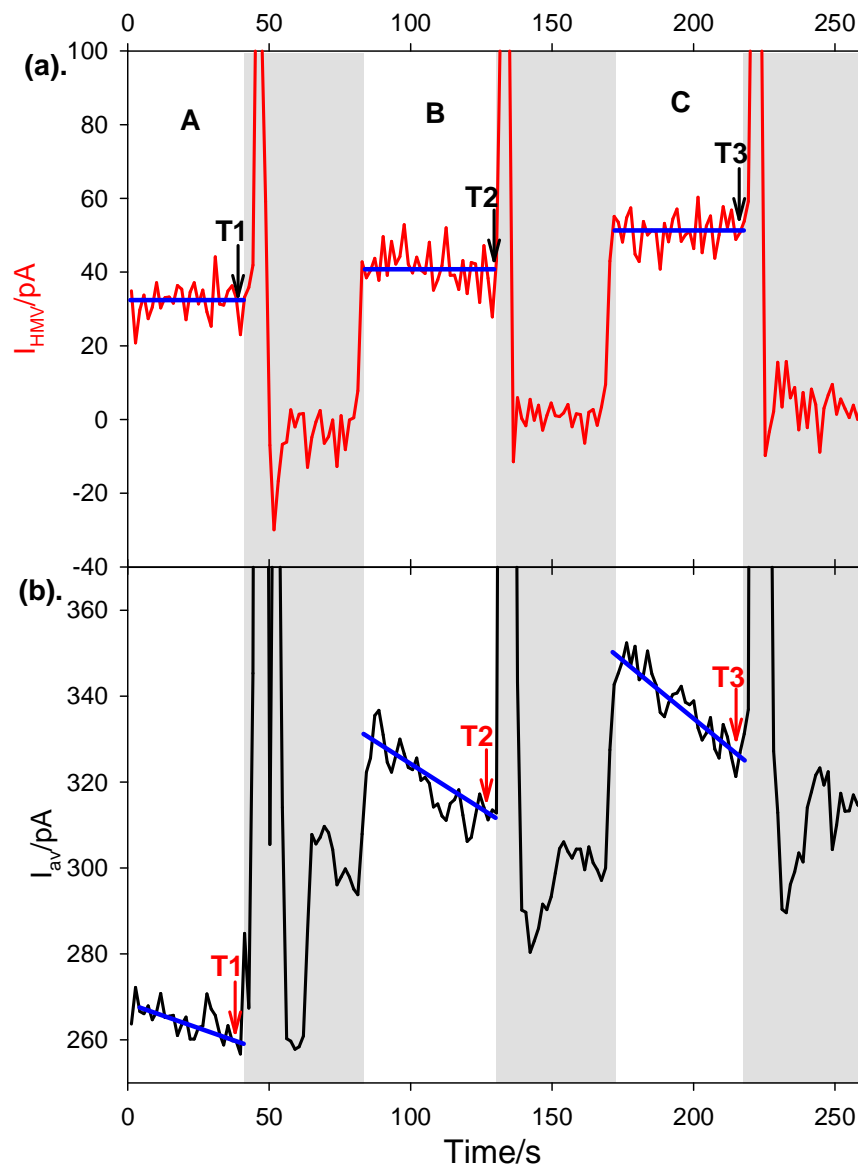
Figure 1
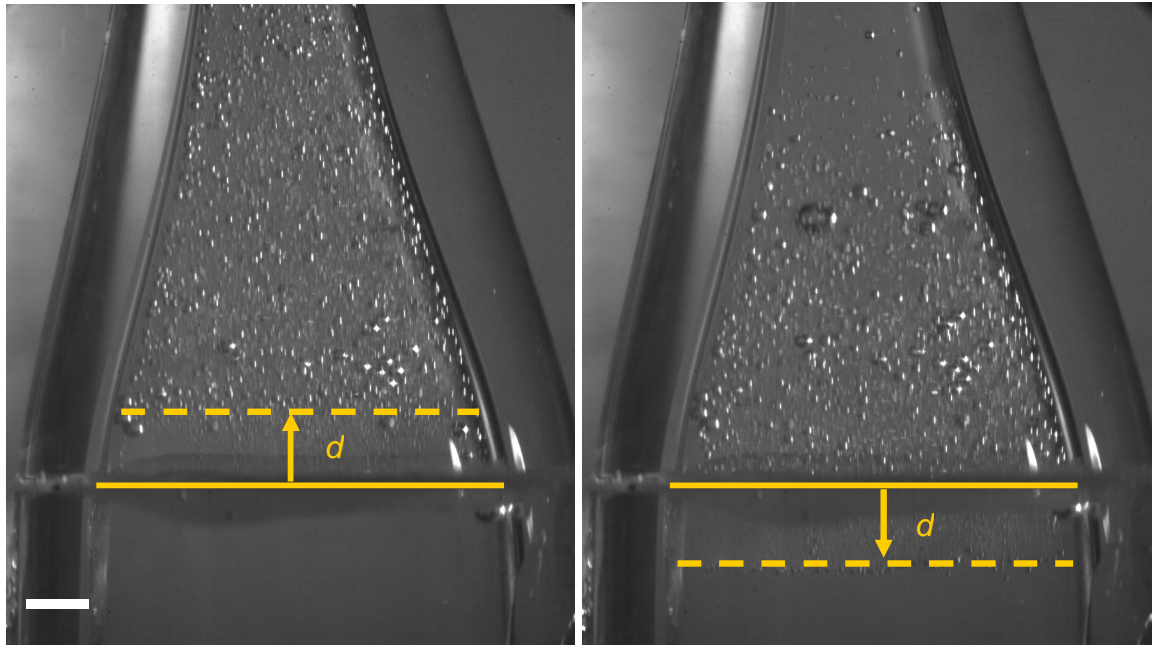
Figure 2
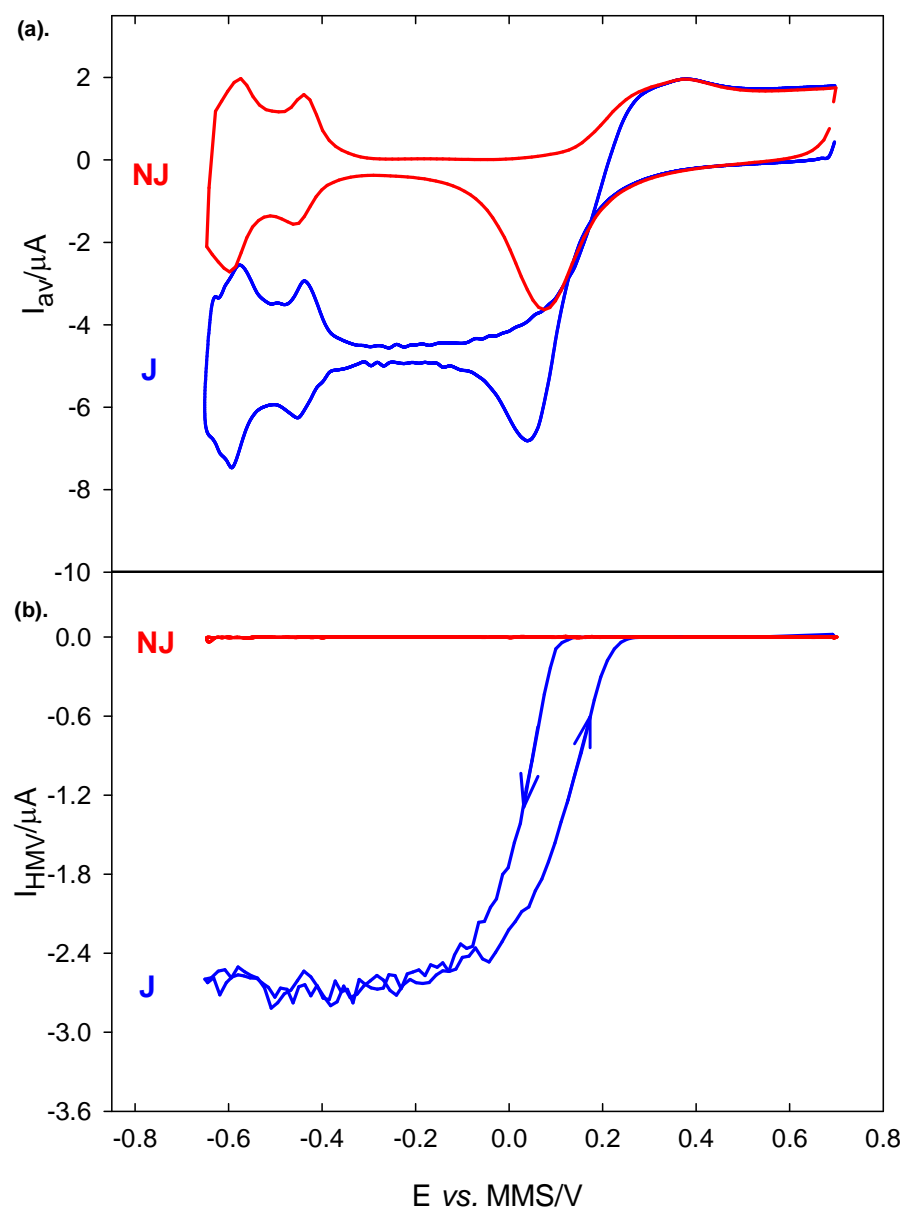
Figure 3
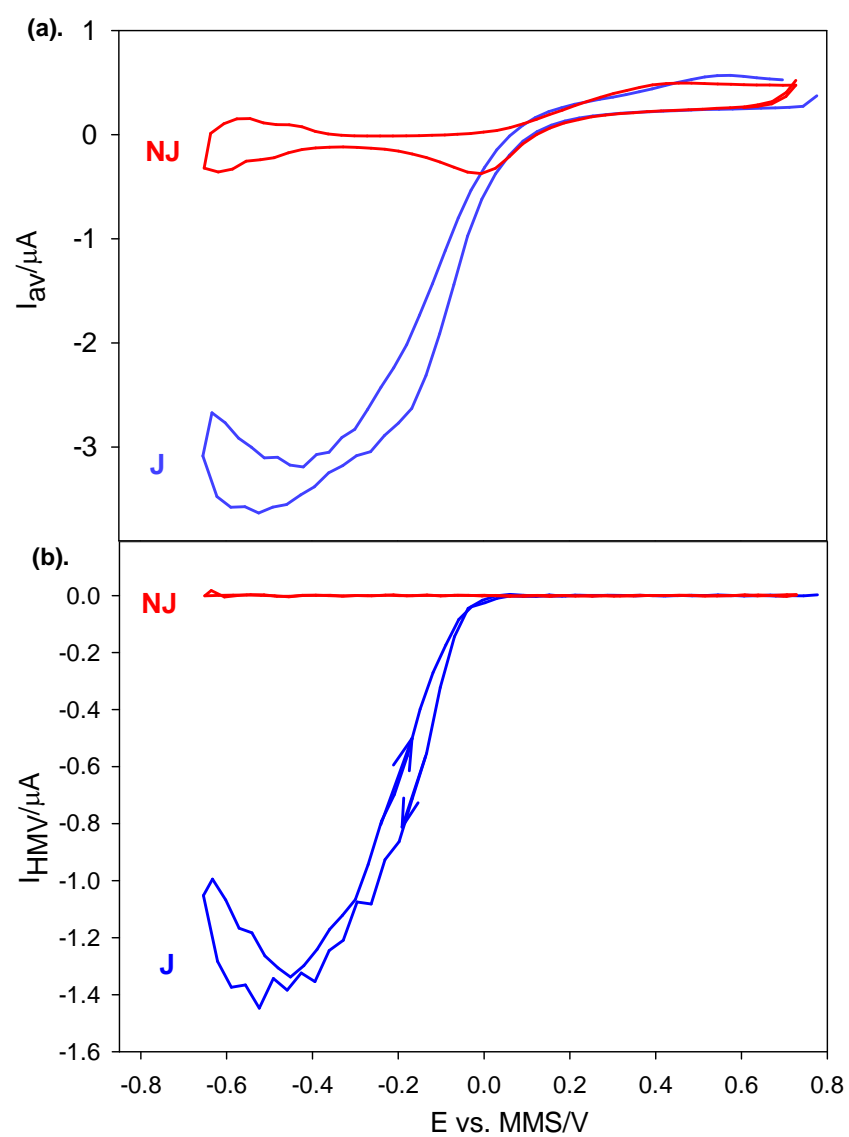
Figure 4.

Figure 5

References

[1]   P. R. Birkin, J. M. Elliott, Y. E. Watson, Chem. Commun. (2000) 1693.

[2]   O. Antoine, R. Durand, J. Appl. Electrochem. 30 (2000) 839.

[3]   S. A. G. Evans, J. M. Elliott, L. M. Andrews, P. N. Bartlett, P. J. Doyle, G. Denuault, Anal. Chem. 74 (2002) 1322.

[4]   A. Schneider, L. Colmenares, Y. E. Seidel, Z. Jusys, B. Wickman, B. Kasemo, R. J. Behm, Phys. Chem. Chem. Phys. 10 (2008) 1931.

[5]   V. R. Stamenkovic, B. Fowler, B. S. Mun, G. F. Wang, P. N. Ross, C. A. Lucas, N. M. Markovic, Science 315 (2007) 493.

[6]   J. M. Elliott, P. R. Birkin, P. N. Bartlett, G. S. Attard, Langmuir 15 (1999) 7411.

[7]   A. J. Bard, L. R. Faulkner, Electrochemical Methods. Fundamentals and Applications., second ed., John Wiley & Sons, Inc., 2001.

[8]   R. N. Adams, Electrochemistry at Solid Electrodes, Marcel Dekker, Inc., New York, 1969.

[9]   J. Wang, Talanta 28 (1981) 369.

[10]   J. V. Macpherson, Electroanalysis 12 (2000) 1001.

[11]   B. Miller, S. Bruckenstein, Anal. Chem. 46 (1974) 2026.

[12]   S. A. Schuette, R. L. McCreery, Anal. Chem. 58 (1986) 1778.

[13]   J. V. Macpherson, P. R. Unwin, Anal. Chem. 71 (1999) 2939.

[14]   J. V. Macpherson, P. R. Unwin, Anal. Chem. 71 (1999) 4642.

[15]   G. S. Attard, P. N. Bartlett, N. R. B. Coleman, J. M. Elliott, J. R. Owen, J. H. Wang, Science 278 (1997) 838.

[16]   T. Imokawa, K. J. Williams, G. Denuault, Anal. Chem. 78 (2006) 265.

[17]   M. Y. Nie, J. M. Elliott, J. Mater. Sci. 21 (2005) 863.

[18]   P. V. Braun, P. Osenar, S. I. Stupp, Nature 380 (1996) 325.

[19]   A. H. Whitehead, J. M. Elliott, J. R. Owen, in 9th International Meeting on Lithium Batteries, Elsevier Science Sa, Edinburgh, Scotland, 1998, pp. 33.

[20]   J. J. Jiang, A. Kucernak, Electrochem. Solid-State Lett. 3 (2000) 559.

[21]   W. J. Blaedel, J. Wang, Anal. Chem.51 (1979) 799.

[22]   N. Simjee, P. R. Unwin, J. V. Macpherson, Electroanalysis 15 (2003) 1445.

[23]   K. W. Pratt, D. C. Johnson, Anal. Chim. Acta 148 (1983) 87.

[24]   W. J. Blaedel, R. C. Engstrom, Anal. Chem. 50 (1978) 476.

[25]   W. J. Blaedel, J. Wang, Anal. Chem. 52 (1980) 1697.

[26]   B. Miller, S. Bruckenstein, J. Electrochem. Soc. 121 (1974) 1558.

[27]   B. Miller, J. M. Rosamilia, Abstracts of Papers of the American Chemical Society 186 (1983) 44.

[28]   J. Kuleshova, P. R. Birkin, J. M. Elliott, J. Electroanal. Chem. 617 (2008) 185.

[29]   J. Kuleshova, PhD Thesis, School of Chemistry, University of Southampton, 2008.

[30]   J. M. Elliott, G. S. Attard, P. N. Bartlett, N. R. B. Coleman, D. A. S. Merckel, J. R. Owen, Chem. Mater. 11 (1999) 3602.

[31]   H. Angersteinkozlowska, B. E. Conway, W. B. A. Sharp, J. Electroanal. Chem. 43 (1973) 9.

[32]   F. G. Will, C. A. Knorr, Zeitung Elektrochemie 64 (1960) 258.

[33]   R. Parsons, in: R. G. Compton and A. Hamnett (Eds.), Comprehensive Chemical Kinetics, 29, Elsevier, Amsterdam, 1989, pp. 105-127.

[34]   B. E. Conway, Prog. Surf. Sci. 49 (1995) 331.

[35]   M. R. Tarasevish, A. Sadkowski, E. Yeager, in: B. E. Conway, J. O. Bockris, E. Yeager, S. U. M. Khan, and R. E. White (Ed.), Comprehensive Treatise of Electrochemistry, 7, Plenum Press, New York, 1983, pp. 301.

[36]   G. Jerkiewicz, G. Vatankhah, J. Lessard, M. P. Soriaga, Y. S. Park, Electrochim. Acta 49 (2004) 1451.

[37]   D. Pletcher, S. Sotiropoulos, J. Electroanal. Chem. 356 (1993) 109.

[38]   S. Chen, A. Kucernak, J. Phys. Chem. B 108 (2004) 3263.

[39]   Manufacturer supplied data.

[40]   C. Beriet, D. Pletcher, J. Electroanal. Chem. 361 (1993) 93.

[41]   J. C. Miller, J. N. Miller, Statistics for Analytical Chemistry, third ed., Ellis Horwood, New York, 1993.